APOD-Based Control of Linear Distributed Parameter Systems Under Sensor/Controller Communication Bandwidth Limitations

Davood Babaei Pourkargar and Antonios Armaou
Dept. of Chemical Engineering, The Pennsylvania State University, University Park, PA 16802

DOI 10.1002/aic.14640
Published online October 20, 2014 in Wiley Online Library (wileyonlinelibrary.com)

The synthesis of a model-based control structure for general linear dissipative distributed parameter systems (DPSs) is explored in this manuscript. Discrete-time distributed state measurements (called process snapshots) are used by a continuous-time regulator to stabilize the process. The main objective of this article is to identify a criterion to minimize the communication bandwidth between sensors and controller (snapshots acquisition frequency) using linear systems analysis and still achieve closed-loop stability. This objective is addressed by adding a modeling layer to the regulator. Theoretically, DPSs can be well described by low dimensional ordinary differential equation models when represented in functional spaces; practically, the model accuracy hinges on finding basis functions for these spaces. Adaptive proper orthogonal decomposition is used to identify statistically important basis functions and establish locally accurate reduced order models which are then used in controller design. The proposed approach is successfully applied toward thermal regulation in a tubular chemical reactor. © 2014 American Institute of Chemical Engineers *AIChE J*, 61: 434–447, 2015

Keywords: distributed parameter systems, adaptive model reduction, adaptive proper orthogonal decomposition, process control, hybrid systems

Introduction

There are many industrial chemical engineering processes that display strong spatial variation due to the interplay of transport and reaction phenomena. Representative examples of important diffusion-convection-reaction processes in chemical industries include catalytic reactors, lithographic operations, crystallization, and polymerization processes.[1–4] The spatiotemporal behavior of aforesaid processes generally takes the form of dissipative partial differential equations (PDEs). One of the effective methods to address monitoring, control, and optimization of such systems is via model order reduction (MOR).[5–8] In MOR approaches, the PDE system is represented as an infinite set of ordinary differential equations (ODEs) using the method of weighted residuals based on analytically computed basis functions. Then according to the type of PDE, usually a proper separation between the set of ODEs can be found to approximate the infinite dimensional system with a set of finite dimensional ODEs that capture the dominant dynamic of the system. Most of the approaches in this category are analytical methods that are only applicable to quasilinear PDEs.[7]

The applicability of analytical model reduction methods in industrial processes is limited due to complex nonlinear spatial dynamics and irregular domains. Even for linear distributed parameter systems (DPSs) in their general form, analytical approaches may be inapplicable to construct the reduced order model (ROM). The significant difficulty arises in computing the set of basis functions which are needed for MOR. To circumvent this limitation, statistical techniques are used to construct the required empirical basis functions.[1,9–13]

Principal component analysis methods and specifically proper orthogonal decomposition (POD) techniques are extensively applied to obtain the set of empirical basis functions for spatial profiles using orthogonal transformation to convert an ensemble of possibly correlated data into a set of linearly independent and uncorrelated components.[13] Various POD-like methods subsequently use this key idea to find relevant basis functions and construct the ROM for estimation and control of DPSs.[1,9,11,14–17] The POD-like approaches have the typical limitation of statistical pattern analysis methods, that is they assume that a sufficient large ensemble of solution data is available that contains all of the excited modes and their significance. These assumptions are practically difficult to be satisfied for most of the systems; to circumvent this issue the adaptive version of POD was introduced.[18] Adaptive proper orthogonal decomposition (APOD) is used when additional data (snapshots) from the system becomes available during process progression to recursively update the set of empirical basis functions. It was shown that the APOD algorithm leads to a threefold increase in computational speed compared to on-line POD-like methods and similar optimization based techniques.[12] The APOD-based estimation problem was briefly addressed where the requirements on continuous measurement sensors is reduced via dynamic

Correspondence concerning this article should be addressed to: A. Armaou at armaou@engr.psu.edu.

observer designs.[19] Recently, a modified APOD was tailored for fast transient DPSs that uses the Shanon entropy of the ensemble.[10] The motivation of the modified approach is based on a new ensemble revision strategy to obtain a semiglobally valid set of empirical basis functions. Geometric output feedback controllers were designed to track the desired output of the system.[20,21] Also, gappy-APOD was introduced to address the control and estimation of spatially distributed processes in the presence of periodic distributed measurement constraints.[22]

One of the remaining unanswered questions in APOD-based control problem of DPSs is how one can identify the required frequency for ROM revisions. The required time interval between the ROM revisions and as a result the frequency of snapshots in the APOD-based control should satisfy closed-loop stability criteria. For DPSs, we observe that increasing the time interval between revisions reduces the communication load and the spatially distributed measurement costs but it may inadvertently affect closed-loop system stability as it will be shown in this article. The revision time influence on stability has been considered for ODE systems.[23] and PDE systems[24]; the tailored APOD-specific analysis for DPSs will be illustrated in "Closed-loop system analysis" section. Considering such trade-off between stability and measurement costs, obtaining snapshots at a proper frequency is one of the most important prerequisites of APOD-based controller designs.

In the current work, we consider the set of sensors (that acquire information), controller structure (that analyzes process information, revises the ROM and computes the required action), and actuators (that enforce that command) as a small communication network with a limited bandwidth for closed-loop process data transfer. Using such conceptual duality between finding the required revision time intervals for APOD-based control and desired feedback frequency for control of networked systems in the presence of communication constraints can be extremely helpful as communication networks are well studied theoretically and are extensively used in the distributed and networked control of advanced chemical processes for fast dissemination of information between operators. When control system elements communication bandwidth is limited, improved methods are needed for state estimation and controller design to overcome the communication constraints (see Ref. 25 and references therein). Recently, networked model-based control of lumped systems has been studied in detail (see Ref. 23 and references therein), while networked controllers that circumvent the sensor-controller communication constrains in DPSs has been investigated.[24,26–28] We use the concepts behind networked control method to identify criteria that guarantee system closed-loop stability and in this way we address the spatially distributed measurements frequency problem of APOD.

To achieve our goals in minimizing the frequency of snapshots (minimizing ROM revisions), we apply a similar approach to the networked feedback controller designs for DPSs.[27] The controller was synthesized for dissipative DPSs which can be discretized to finite dimensional slow (and possibly unstable) and infinite-dimensional fast subsystems when represented in appropriate Sobolev spaces. The slow subsystem model is included in the control structure to reduce the frequency of sensor measurements over the network when communication is suspended. To compute the smallest frequency at which communication must be reestablished and the ROM must be updated, the concepts of networked control for linear systems have been used. A criterion is then identified for minimizing communication bandwidth (snapshots transfer rate) from the periodic measurement sensors to the controller considering closed-loop stability. "Mathematical Preliminaries" section introduces mathematical concepts used through the article. A short review on adaptive model reduction is presented in "Adaptive model reduction" section. It includes the off-line and on-line computation of empirical basis functions and ROM construction. The APOD-based control system is described in "Control system" section, where the criterion is obtained for minimizing the communication bandwidth. Finally, in "Simulation results" section the proposed control structure is successfully illustrated on thermal dynamic regulation in a tubular chemical reactor.

Mathematical Preliminaries

Consider a linear DPS with a state space description of dissipative linear PDEs of

$$\begin{aligned} &\frac{\partial}{\partial t}X(z,t)=\mathbf{A}(z)X(z,t)+b(z)u(t),\\ &s.t.\ q\left(X,\frac{\partial X}{\partial z},...,\frac{\partial^{n-1}X}{\partial z^{n-1}}\right)=0 \text{ on } \partial\Omega,\ X(z,0)=X_0(z). \end{aligned} \tag{1}$$

We define the snapshot measurements as discrete-time full state measurements, mathematically expressed by

$$y(z,t_k)=\int_0^t \delta(\tau-t_k)X(z,\tau)d\tau \tag{2}$$

In the above system, $z\in\Omega$ is the spatial coordinate, $t\in[0,\infty)$ is time and $X(z,t)\in\mathbb{R}$ denotes the state vector of the system. $\Omega\subset\mathbb{R}^3$ is the domain of the process and $\partial\Omega$ is the process boundary, $u\in\mathbb{R}^l$ denotes the manipulated input vector. $\mathbf{A}(z)$ is a linear spatial differential operator of order n, $q(.)$ is a smooth nonlinear vector function and $X_0(z)$ is a smooth vector function of z, $b^T(z)\in\mathbb{R}^l$ is a known smooth vector function of z that describes how manipulated input vector is distributed in the spatial domain Ω, for example, point actuation can be defined using standard Dirac delta and continuous actuation can be described by step functions. We assume the availability of a periodic distributed snapshot measurement sensor, $y(z,t_k)\in\mathbb{R}$, where y indicates measured spatial profiles and t_k is the occurrence time instant for snapshot measurement. The control objective is to regulate the PDE system of (1) at a desired spatial profile, $X_d(z)$. Without loss of generality, the spatially uniform steady state $X_d(z)=0$ is considered as the desired profile.

The PDE system of (1) can be presented as an infinite-dimensional system in a relevant Sobolev space $\mathbf{W}^{(n-1),2}(\Omega,\mathbb{R}),\forall i,j\in\mathbb{N},i\geq 1$ and $1\leq j<\infty$

$$\mathbf{W}^{i,j}=\{\bar{x}\in L^j(\Omega):\ \partial^\alpha\bar{x}\in L^j(\Omega),\forall\alpha\in\mathbb{N},|\alpha|\leq i\}.$$

where Sobolev spaces are functional subspaces that consider functions for which all the distributional derivatives can be applied. We can define the inner product and norm in $L_2(\Omega)$ as

$$(\vartheta_1,\vartheta_2)=\int_\Omega r(z)\vartheta_1^T(z)\vartheta_2(z)dz,\ \ ||\vartheta_1||_2=(\vartheta_1,\vartheta_1)^{1/2},$$

where ϑ^T denotes the transpose of ϑ and $r(z)$ is the weight function that is assumed to be 1 in this work.

We define the state $\bar{x}\in\mathbb{W}^{(n-1),2}$ as

$$\bar{x}(t)=X(z,t), \tag{3}$$

the linear differential operator

$$\mathcal{A}\bar{x}=\mathbf{A}(z)X, \tag{4}$$

and the manipulated input as $\mathcal{B}u=b(z)u$, where $\mathbb{W}^{(n-1),2}(\Omega, \mathbb{R})$ is a Sobolev subspace that satisfies the homogeneous boundary conditions of (1), that is

$$\mathbb{W}^{(n-1),2}(\Omega,\mathbb{R})=\left\{f\in\mathbf{W}^{(n-1),2}(\Omega,\mathbb{R}):\ q\left(f,\frac{\partial f}{\partial z},...,\frac{\partial^{n-1}f}{\partial z^{n-1}}\right)=0 \text{ on } \partial\Omega\right\}.$$

Then the PDE system of (1) can be presented in the Sobolev subspace as follows

$$\dot{\bar{x}}=\mathcal{A}\bar{x}+\mathcal{B}u,\ \ \bar{x}(0)=\bar{x}_0. \tag{5}$$

Note that to simplify the notation we will use $\mathbb{W}$ to denote $\mathbb{W}^{(n-1),2}(\Omega,\mathbb{R})$ in the rest of the article.

In the analytical model reduction approaches, the set of basis functions of the system, needed to build ROMs, can be obtained from the solution of the eigenvalue problem for the linear spatial operator of $\mathcal{A}$, as follows

$$\mathcal{A}\phi_i=\lambda_i\phi_i,\ \ \phi_i\in\mathbb{W}, i=1,\ldots,\infty. \tag{6}$$

where λ_i and ϕ_i denote the ith eigenvalue and the corresponding basis function, respectively. Note that ϕ_i is a complete basis of $\mathbb{W}$ for self adjoint operators.

Assumption 1. *Consider the ordered eigenspectrum of $\mathcal{A}$ as $\sigma_{\mathcal{A}}=\{\lambda_1,\lambda_2,\ldots\}$ where*

$$\mathrm{Re}(\lambda_1)\geq\mathrm{Re}(\lambda_2)\geq\cdots$$

and $\mathrm{Re}(\lambda)$ *denotes real part of λ. We assume that $\sigma_{\mathcal{A}}$ can be partitioned into a finite dimensional set of α slow eigenvalues, $\sigma_{\mathcal{A}}^{(s)}=\{\lambda_1,\lambda_2,\ldots,\lambda_\alpha\}$, and a stable infinite-dimensional complement set of the remaining fast eigenvalues $\sigma_{\mathcal{A}}^{(f)}=\{\lambda_{\alpha+1},\lambda_{\alpha+2},\ldots\}$. The associated basis functions sets are defined as $\Phi_s=[\phi_1\ \phi_2\ \cdots\ \phi_\alpha]^T, \Phi_f=[\phi_{\alpha+1}\ \phi_{\alpha+2}\ \cdots]^T$. There is a large separation between the slow and fast eigenvalues of $\mathcal{A}$, that is, $|\mathrm{Re}(\lambda_1)|/|\mathrm{Re}(\lambda_\alpha)|=O(1)$ and $|\mathrm{Re}(\lambda_1)|/|\mathrm{Re}(\lambda_{\alpha+1})|=O(\gamma)$ where $\mathrm{Re}(\lambda_{\alpha+1})<0, \gamma=|\lambda_1|/|\lambda_{\alpha+1}|$ is a small number and $O(\gamma)$ indicates the order of γ.*

According to Assumption 1, the system Sobolev subspace, $\mathbb{W}\triangleq\mathrm{span}\{\phi_i\}_{i=1}^{\infty}$, can be partitioned into two Sobolev subspaces, named slow and fast subspaces, $\mathbb{W}_s$ and $\mathbb{W}_f$, respectively, where $\mathbb{W}=\mathbb{W}_s\oplus\mathbb{W}_f$. The slow subspace includes a finite number of basis functions that correspond to the slow and possibly unstable modes of $\bar{x}$, $\mathbb{W}_s\triangleq\mathrm{span}\{\phi_i\}_{i=1}^{\alpha}$, and the fast complement subspace contains an infinite number of basis functions that correspond to the fast and stable modes of $\bar{x}$, $\mathbb{W}_f\triangleq\mathrm{span}\{\phi_i\}_{i=\alpha+1}^{\infty}$. Then the state of the infinite-dimensional system of (1) can be partitioned into a finite number of slow and possibly unstable modes and an infinite number of stable and fast modes with respect to the basis of the Sobolev subspace, $\mathbb{W}$

$$\bar{x}=\bar{x}_s+\bar{x}_f, \tag{7}$$

where $\bar{x}_s=\mathcal{P}\bar{x}\in\mathbb{W}_s$ and $\bar{x}_f=\mathcal{Q}\bar{x}\in\mathbb{W}_f$. The orthogonal integral projection operators are defined as $\mathcal{P}:\mathbb{W}\rightarrow\mathbb{W}_s, \mathcal{P}=(\cdot,\Phi_s)$ and $\mathcal{Q}:\mathbb{W}\rightarrow\mathbb{W}_f, \mathcal{Q}=(\cdot,\Phi_f)$.

From (7) and using the method of weighted residuals based on the set of basis functions, the system of (5) can be presented as a partitioned ODE set of vectorized modes in the following form

$$\begin{aligned}\dot{\bar{x}}_s&=A_s\bar{x}_s+B_su,\bar{x}_s(0)=\mathcal{P}\bar{x}_0,\\ \dot{\bar{x}}_f&=A_f\bar{x}_f+B_fu,\bar{x}_f(0)=\mathcal{Q}\bar{x}_0,\end{aligned} \tag{8}$$

where $A_s=\mathcal{P}\mathcal{A}, A_f=\mathcal{Q}\mathcal{A}, B_s=\mathcal{P}\mathcal{B}, B_f=\mathcal{Q}\mathcal{B}, \mathcal{P}\bar{x}(0)=\mathcal{P}\bar{x}_0, \mathcal{Q}\bar{x}(0)=\mathcal{Q}\bar{x}_0, X=X_s+X_f, X_s=\Phi_s^T\bar{x}_s$ and $X_f=\Phi_f^T\bar{x}_f$. Note that in above modal expansions, $A_s=\mathrm{diag}\{\lambda_i\}_{i=1}^{\alpha}$ and $A_f=\mathrm{diag}\{\lambda_i\}_{i=\alpha+1}^{\infty}$ are diagonal matrices. Also, as there is an order of magnitude difference between $\mathrm{Re}(\lambda_1)$ and $\mathrm{Re}(\lambda_{\alpha+1})$, then there is a time scale separation between the dynamic behavior of the two subsystems.

On the basis of the above discussion, to implement the analytical model reduction we need to solve the eigenvalue problem of (6) and find the set of basis functions. However, generally it is not possible to solve it when we have complex boundary conditions. The interesting fact is that we can not find the analytical solution even for a general class of linear systems over miscellaneous domains. Thus, most of the standard analytical model reduction techniques can not be directly used even for DPSs described by general linear PDEs. One solution to circumvent this issue is to apply APOD as explained briefly in the introduction section.

Remark 1. *The results in this work are presented for $X\in\mathbb{R}$, however, it is straightforward to extend the results for $X\in\mathbb{R}^m$ by treating each state individually and combining the resulting ODE descriptions. Once each PDE has been reduced, the interactions between distributed system states can be easily captured from their modal expansions.*[13]

Remark 2. *The assumption of large separation between slow and fast dynamics of the system (Assumption 1) is satisfied by wide range of transport-reaction processes (see Ref.* 29 *for heating rod and catalytic packed-bed reactor examples, Refs.* 30–32 *for chemical vapor deposition process and Ref.* 33 *for plasma discharge reactor). Assumption 1 is fundamental to the existence of only a few dominant modes that can describe the dominant dynamic behavior of the parabolic PDE system. Based on this assumption, we can approximate the* DPS *by a finite dimensional ODEs.*

Adaptive Model Reduction

Adaptive proper orthogonal decomposition

The flow chart of APOD including its algebraic steps is presented in Figure 1. For brevity reasons, we only review the key steps in the flow chart in this article. A detailed analysis of the key features of the off-line and on-line parts of the algorithm can be found in Refs. 10,12.

The off-line steps of the APOD can be summarized as follows,

- Ensemble construction: Let $v=\{\bar{x}(z,t_k)\}_{k=1}^{K}$ be the ensemble in vector form, where $\bar{x}(z,t_k)$ denotes the snapshot of the system state available at time t_k which is $y(z,t_k)$.
- Z computation: Compute the covariance matrix of the ensemble, $C_K:=(v^T,v^T)$ and identify the smallest r such that $\sum_{i=1}^{r}\lambda_i/\sum_{i=1}^{K}\lambda_i\geq\varepsilon$, where ε is an operator parameter. Order the eigenvalues in terms of size. An orthonormal basis is obtained as $Z=[\omega_1\ \omega_2\ \cdots\ \omega_r], Z\in\mathbb{R}^{K\times r}$ where ω_i denotes the ith eigenvector of C_K that corresponds to the ith eigenvalue, λ_i.
- Basis functions construction: Defining diagonal matrix of $\Lambda=[\lambda_i\delta_{ij}]_{ij}$, $i,j=1,\ldots,r$, compute the vector of basis

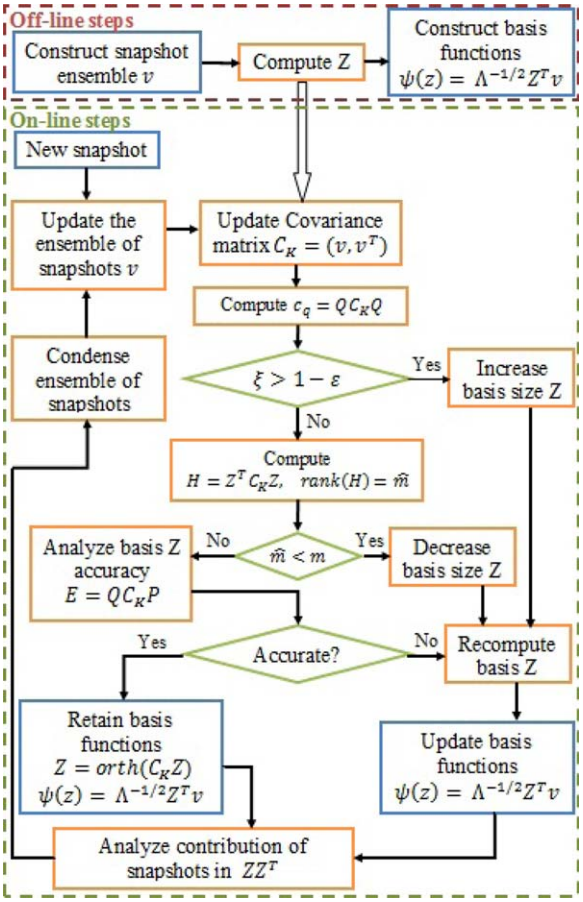

Figure 1. Flow chart of APOD.[10]

[Color figure can be viewed in the online issue, which is available at wileyonlinelibrary.com.]

functions, $\Psi=[\psi_1\ \psi_2\ \cdots\ \psi_r]^T$, as $\Psi=\Lambda^{-1/2}Z^T v$ where δ_{ij} is the Kronecker delta.

The on-line steps of the APOD can also be summarized as follows,

- Ensemble updating: To construct an ensemble that retains the most important snapshots at each revision time instant, eliminate the snapshot with the lowest value in the normalized snapshot contribution matrix in ZZ^T (refer to[10] for details). Then update the resulting ensemble by adding the new snapshot.
- Update the covariance matrix, C_K.
- Compute $c_q = QC_KQ$, $\xi=\lambda_{r+1}/\sum_{i=1}^{r+1}\lambda_i$ and $H=Z^TC_KZ$.
- Decision: Increase, decrease or retain the order of Z.[12]
- Updating the basis functions: If increasing or decreasing Z, the basis functions are updated based on new Z as $\Psi=\Lambda^{-1/2}Z^Tv$.
- Accuracy analysis: $E=QC_{KP}$, where $P=ZZ^T$ and $Q=I-ZZ^T$.
- Retaining the basis functions: If retaining Z, we revise it as $Z=\text{orth}(C_KZ)$ and update the basis functions based on revised Z.

Finite dimensional approximation using the method of weighted residuals

The finite-dimensional approximation of the infinite-dimensional PDE system of (1) can be presented in the form of an ODE set of slow and possibly unstable modes using the method of weighted residuals if and only if we have a "proper" (defined in the next section) set of analytical or empirical basis functions. The state of the original PDE system of (1), $X(z, t)$, can be recast as an infinite weighted sum of a complete set of basis functions, $\psi_k(z)$, as

$$X(z,t)=\sum_{k=1}^{\infty}x_{m,k}(t)\psi_k(z). \tag{9}$$

Then the following approximation can be obtained by truncating the series expansion of $X(z, t)$ up to order r

$$\hat{X}(z,t)=\sum_{k=1}^{r}x_{m,k}(t)\psi_k(z), \tag{10}$$

where r is the number of slow modes and $x_m(t)$ denotes time varying coefficients known as system modes. The following ODE set of order r is obtained by substituting (10) in (1), multiplying the PDE with the weighting functions, $\varphi(z)$, and integrating over the entire spatial domain

$$\begin{aligned}\sum_{k=1}^{r}(\varphi_j(z),\psi_k(z))\dot{x}_{m,k}(t)&=\sum_{k=1}^{r}(\varphi_j(z),\mathcal{A}(z)\psi_k(z))x_{m,k}(t)\\&+(\varphi_j(z),b(z))u(t),\quad j=1,\ldots,r\end{aligned} \tag{11}$$

Note that the type of weighted residual method depends on the type of weighting functions used in the above procedure. It is Galerkin's method when the weighting functions, $\varphi(z)$, and the basis functions, $\psi(z)$, are the same. Galerkin's method leads to accurate finite dimensional ODE models for processes that exhibit strong diffusive phenomena and can thus be described by highly dissipative PDE systems; this is due to the fact that their dominant dynamic behavior can be captured by a finite number of dominant spatial profiles. The reduced order system of (11) can be summarized as

$$\dot{x}_m=A_mx_m+B_mu. \tag{12}$$

This system is considered for control design purposes in the next section.

Control system

In this section, we consider the control problem of general linear DPSs the spatiotemporal dynamics of which can be described in the form of (1). We use the idea of networked control approach to regulate the system and seek appropriate criteria for frequency of periodic spatially distributed measurements considering closed-loop stability. Note that the open-loop spatially distributed process may be stable or unstable; that does not affect the analysis. We assume there is no delay in snapshot communication from the periodic distributed measurement sensors to ROM and controller. The main objective is to find the smallest frequency at which the ROM must be updated based on the availability of the snapshots from the periodic distributed measurement sensors.

Assumption 2. *The process slow dynamics and as a result the slow subsystem of* (8) *is assumed to be controllable, and spillover to the fast subsystem is of finite magnitude.*

The partitioned dynamics of the real process, the APOD-based switching model and the state feedback controller equation can be summarized as

$$\begin{aligned}\text{Process}:\ \dot{\bar{x}}_s &= A_s\bar{x}_s + B_s u,\\ \dot{\bar{x}}_f &= A_f\bar{x}_f + B_f u,\\ \text{Model}:\ \dot{x}_m &= A_m x_m + B_m u,\\ \text{Controller}:\ u &= \tilde{K}x_m,\end{aligned} \tag{13}$$

where the controller design goal is computing the matrix of $\tilde{K}$ in the state feedback controller equation of $u=\tilde{K}x_m$, such that the eigenvalues of the closed-loop system are placed in predetermined positions.

According to Assumption 2, the slow dynamics of the system of (13) is controllable. Then it is possible to place the closed-loop system poles anywhere in the complex domain, where the poles' locations correspond directly to the eigenvalues of the system[34] We use the ROM and a pole placement technique, for example Ackermann's formula, to compute a state feedback controller gain matrix, $\tilde{K}$, that places the closed-loop poles of the system in predetermined locations. As the process evolves, when APOD revises the set of empirical basis functions the structure and size of the ROM may change. These changes directly affect the controller structure. In such cases, the controller should be redesigned. We use Butterworth formula to predetermine a set of Hurwitz characteristic polynomials and an ordered set of desired stable poles of closed-loop dynamics before closed-loop operation.[34] When the dimension of ROM changes during process evolution, the controller structure chooses the appropriate number of poles and their predetermined locations.

Remark 3. *Assumption 2 is not as restrictive as may look, since the controllability of DPSs depends on the actuators' locations. In addition, the controllability of the ROM also depends on the discretization method and discretization points.*[35] *Using singular perturbation arguments for Galerkin's method we can link the controllability of ROM with the controllability of DPS. Most of the spatially distributed processes in the chemical industries are over-designed to be controllable by placing the actuators in appropriate locations with respect to open-loop criteria.*[36] *The reader may refer to Refs.* 36,37 *for actuators' placement methods that satisfy controllability of the ROM and DPS and suppress spillover to higher order dynamics.*

Remark 4. *Alternatively we may assume that the infinite-dimensional system of* (5) *is approximately controllable.*[38] *There is a direct relationship between approximate controllability and exact controllability of the slow subsystem. Assumption 2 is less restrictive than this requirement because approximate controllability even though is not enforcing exact controllability to the system, it assumes that the fast subsystem is also controllable which is not the case of the assumption.*

Closed-loop system analysis

The slow and dominant part of the state in the original PDE system of (1) can be defined as follows

$$X_s(z,t)=\Phi_s^T(z)\bar{x}_s(t). \tag{14}$$

Also the model state of the PDE system is obtained by

$$\hat{X}(z,t)=\Psi^T(z)x_m(t), \tag{15}$$

where $\Psi=[\psi_1\psi_2\ldots\psi_r]^T, \Phi_s=[\phi_1\phi_2\ldots\phi_\alpha]^T$; r is the number of empirical basis functions of the slow subsystem that is computed using APOD and α is the number of analytical basis functions of the slow subsystem. Note that we do not require Φ_s for the implementation of the proposed method, we need it just for the stability and performance analysis.

After the fast dynamics have relaxed, that is, $\bar{x}_f \to 0$, the model error can not be defined directly by the simple subtraction, $\bar{x}_s - x_m$ because the dimension of the system slow modes, $\bar{x}_s$ and APOD-based modes, x_m, in (13) is not necessarily the same since the number of identified slow subsystem basis functions Φ_s and Ψ can be different. Thus, we need a transformation to project one subspace to other and define the projected error.

Assumption 3. *Consider the local subspace of the slow and unstable modes,* $\mathbb{W}_s \triangleq \text{span}\{\phi_i\}_{i=1}^{\alpha}$ *and subspace* $\mathbb{P}$ *defined as* $\mathbb{P} \triangleq \text{span}\{\psi_i\}_{i=1}^{r}$, *where* $\{\phi_i\}_{i=1}^{\alpha}$ *is the set of analytical basis functions of the slow subsystem (which are unavailable) and* $\{\psi_i\}_{i=1}^{r}$ *is the set of empirical basis functions (computed based on APOD). The complement subspace of* $\mathbb{P}$ *can also be defined as* $\mathbb{Q} \triangleq \text{span}\{\psi_i\}_{i=r+1}^{\infty}$. *We assume that* $\mathbb{W}_s \subseteq \mathbb{P}$, *locally*.

Note that Assumption 3 is justified based on the excitation of the higher modes and reordering of the modes during the closed-loop process evolution. The problem with linear systems is that due to subsampling the empirical basis functions and modes may not be properly ordered. One solution to bridge slow Sobolev subspace $\mathbb{W}_s$ and subspace $\mathbb{P}$ is by defining a bounded mapping between these two subspaces to find the corresponding states. The map should be defined as a linear transformation that changes at ROM revisions to conserve all of the subspaces' properties during system evolution. Then, from (15) we can define a bounded map between two subspaces, $\mathbb{W}_s$ and $\mathbb{P}$ as follows

$$X_s=\Phi_s^T\bar{x}_s=\Psi^T\mathcal{M}\bar{x}_s=\Psi^T x_p, \tag{16}$$

where $x_p=\mathcal{M}\bar{x}_s, \mathcal{M}:\mathbb{W}_s\mapsto\mathbb{P}$ and

$$\mathcal{M}=(\Psi^T,\Phi_s^T). \tag{17}$$

Note that $\mathcal{M}:\mathbb{W}_s\mapsto\mathbb{P}$, is injective due to the fact that subspace $\mathbb{P}$ contains subspace $\mathbb{W}_s$. Then $x_{p,1}=x_{p,2}, \forall x_{p,1}, x_{p,2} \in \mathbb{P}$ implies that $\bar{x}_{s,1}=\bar{x}_{s,2}, \forall \bar{x}_{s,1}, \bar{x}_{s,2} \in \mathbb{W}_s$. To complete the analysis, the bounded reverse map can be defined as $\mathcal{M}^{\perp}=(\Phi_s^T,\Psi^T), \mathcal{M}^{\perp}:\mathbb{P}\mapsto\mathbb{W}_s$ such that $\mathcal{I}=\mathcal{M}^{\perp}\mathcal{M}:\mathbb{W}_s\mapsto\mathbb{W}_s$ is a bijective map. An interesting fact about this transformation is that $\mathcal{M}^{\perp}=\mathcal{M}^T$.

Using the above transformation, the system modes of the process slow dynamics in (13) can be expressed using the basis functions of subspace $\mathbb{P}$ in the following form

$$\dot{x}_p=A_p x_p+B_p u, \tag{18}$$

where $A_p=\mathcal{M}A_s\mathcal{M}^{\perp}$ and $B_p=\mathcal{M}B_s$.

Now we can define the error based on the difference between states of the process of (18) and the model of (13) as follows

$$e=x_p-x_m. \tag{19}$$

Then the reduced system dynamics can be obtained for $t\in[t_i,t_{i+1}]$ in terms of process and error state

$$\begin{cases}\dot{x}_p=(A_p+B_p\tilde{K})x_p-(B_p\tilde{K})e\\ \dot{e}=(A_e+B_e\tilde{K})x_p+(A_m-B_e\tilde{K})e\end{cases} \tag{20}$$

where the model is revised every δ_t s based on the state profile information from spatially distributed sensors at t_i, that is, $e(t_i)=0$ and we have $\delta_t=t_{i+1}-t_i$. $A_e=A_p-A_m$ and $B_e=B_p-B_m$ are the modeling error matrices that represent the difference between plant and model structures. In linear

systems, the only reason for system deviation can be the modeling error due to sampling which causes an erroneous ordering of the empirical basis functions; basically the empirical eigenvalues have significant deviation from the operator eigenvalues. Once the model starts diverging from the system, APOD revises it.

Defining $x=\left[\begin{smallmatrix}x_p\\ e\end{smallmatrix}\right]$, the system of (20) can be summarized as the following networked system

$$\dot{x}=\mathcal{G}x, \tag{21}$$

where $\mathcal{G}=\begin{bmatrix}A_p+B_p\tilde{K} & -B_p\tilde{K}\\ A_e+B_e\tilde{K} & A_m-B_e\tilde{K}\end{bmatrix}$ and $x(t_i)=\begin{bmatrix}x_p(t_i)\\ 0\end{bmatrix}$ for $t\in[t_i,t_{i+1}]$. Now we can derive the criteria for stability of the networked system.

Proposition 1. *The system of* (21) *with the initial condition of* $x_0=x(t_0)=\begin{bmatrix}x_p(t_0)\\ 0\end{bmatrix}$ *has the following solution*

$$x(t)=e^{\mathcal{G}(t-t_i)}\mathcal{S}^i x_0, \tag{22}$$

where $\mathcal{S}=\begin{bmatrix}I & 0\\ 0 & 0\end{bmatrix}e^{\mathcal{G}\delta_t}\begin{bmatrix}I & 0\\ 0 & 0\end{bmatrix}$ *and* $t\in[t_i,t_{i+1}]$ *(Proposition 1 in Ref. 23).*

Sketch of proof. The solution of the system for $t\in[t_i,t_{i+1}]$ is

$$x(t)=e^{\mathcal{G}(t-t_i)}x(t_i).$$

When resetting the error to zero at t_i, we can restate $x(t_i)$ as

$$x(t_i)=\begin{bmatrix}I & 0\\ 0 & 0\end{bmatrix}x(t_i^-),$$

then we obtain that

$$x(t_i)=\begin{bmatrix}I & 0\\ 0 & 0\end{bmatrix}e^{\mathcal{G}\delta_t}x(t_{i-1}).$$

Finally using initial condition, $x_0=x(t_0)$, the response of the system can be presented as

$$\begin{aligned}x(t)&=e^{\mathcal{G}(t-t_i)}\left(\begin{bmatrix}I & 0\\ 0 & 0\end{bmatrix}e^{\mathcal{G}\delta_t}\right)^i x_0\\ &=e^{\mathcal{G}(t-t_i)}\left(\begin{bmatrix}I & 0\\ 0 & 0\end{bmatrix}e^{\mathcal{G}\delta_t}\begin{bmatrix}I & 0\\ 0 & 0\end{bmatrix}\right)^i x_0.\end{aligned}$$

To proceed we need to analyze the global exponential stability of the system around the origin. The necessary and sufficient conditions for the system to be stable are identified in the following theorem.

Theorem 1. *The solution of the system of* ((21)) *is globally exponentially stable in the neighborhood of* $x=\begin{bmatrix}0\\ 0\end{bmatrix}$ *if and only if the eigenvalues of* $\mathcal{S}=\begin{bmatrix}I & 0\\ 0 & 0\end{bmatrix}e^{\mathcal{G}\delta_t}\begin{bmatrix}I & 0\\ 0 & 0\end{bmatrix}$ *are inside the unit circle (Theorem 1 in Ref. 23).*

Sketch of proof. Taking the two-norm of (21) and using Cauchy-Schwarz inequality we obtain

$$\begin{aligned}||x(t)||_2&=||e^{\mathcal{G}(t-t_i)}\mathcal{S}^i x_0||_2\le||e^{\mathcal{G}(t-t_i)}||_2||\mathcal{S}^i||_2||x_0||_2\\ &\le||e^{\sigma_{\mathcal{G}}^{max}(t-t_i)}||_2||\mathcal{S}^i||_2||x_0||_2\le||e^{\sigma_{\mathcal{G}}^{max}\delta_t}||_2||\mathcal{S}||_2^i||x_0||_2.\end{aligned} \tag{23}$$

where $\sigma_{\mathcal{G}}^{\max}$ is the largest singular value of $\mathcal{G}$. Then it is obvious that the boundedness of the solution only depends on $||\mathcal{S}||_2$ and this term will be bounded if and only if the eigenvalues of $\mathcal{S}$ are inside the unit circle (sufficient condition). To prove the necessity part, assume that the system is stable and $\mathcal{S}$ has at least one eigenvalue outside the unit circle. We consider the exponential term that has the general form of

$$e^{\mathcal{G}T}=\begin{bmatrix}V_1(T) & V_2(T)\\ V_3(T) & V_4(T)\end{bmatrix}.$$

Then the solution value just before the update will be

$$x(t_{i+1}^-)=\begin{bmatrix}V_1(\delta_t)(V_1(\delta_t))^i & 0\\ V_3(\delta_t)(V_1(\delta_t))^i & 0\end{bmatrix}x_0=\begin{bmatrix}(V_1(\delta_t))^{i+1} & 0\\ V_3(\delta_t)(V_1(\delta_t))^i & 0\end{bmatrix}x_0.$$

Since $\mathcal{S}$ has at least one eigenvalue outside the unit circle (in V_1), the solution will grow with i and the system will be unstable.

By defining the transformation matrix, $M_{\text{tr}}=\begin{bmatrix}I & 0\\ I & -I\end{bmatrix}$, we obtain

$$\mathcal{G}^*=M_{\text{tr}}\mathcal{G}M_{\text{tr}}^{-1}=\begin{bmatrix}A_p & B_p\tilde{K}\\ 0 & A_m+B_m\tilde{K}\end{bmatrix}. \tag{24}$$

Then from (24) and the definition of matrix $\mathcal{S}$, we conclude

$$\begin{aligned}\mathcal{S}&=\begin{bmatrix}I & 0\\ 0 & 0\end{bmatrix}e^{\mathcal{G}\delta_t}\begin{bmatrix}I & 0\\ 0 & 0\end{bmatrix}=\begin{bmatrix}I & 0\\ 0 & 0\end{bmatrix}M_{\text{tr}}^{-1}e^{\mathcal{G}^*\delta_t}M_{\text{tr}}\begin{bmatrix}I & 0\\ 0 & 0\end{bmatrix}\\ &=\begin{bmatrix}I & 0\\ 0 & 0\end{bmatrix}e^{\mathcal{G}^*\delta_t}\begin{bmatrix}I & 0\\ I & 0\end{bmatrix}.\end{aligned} \tag{25}$$

If we consider the Laplace transformation of matrix $\mathcal{S}$, we obtain

$$\begin{aligned}\mathcal{L}\{\mathcal{S}\}&=\begin{bmatrix}I & 0\\ 0 & 0\end{bmatrix}\mathcal{L}\{e^{\mathcal{G}^*\delta_t}\}\begin{bmatrix}I & 0\\ I & 0\end{bmatrix}\\ &=\begin{bmatrix}(sI-A_p)^{-1}+(sI-A_p)^{-1}B_p\tilde{K}(sI-A_m-B_m\tilde{K})^{-1} & 0\\ 0 & 0\end{bmatrix},\end{aligned} \tag{26}$$

and only the element of $(sI-A_p)^{-1}+(sI-A_p)^{-1}B_p\tilde{K}(sI-A_m-B_m\tilde{K})^{-1}$ has nonzero eigenvalues. By inverse Laplace transformation we obtain

$$\begin{aligned}&\mathcal{L}^{-1}\{(sI-A_p)^{-1}+(sI-A_p)^{-1}B_p\tilde{K}(sI-A_m-B_m\tilde{K})^{-1}\}\\ &=\mathcal{L}^{-1}\{(sI-A_p)^{-1}(sI-A_m-B_m\tilde{K}+B_p\tilde{K})(sI-A_m-B_m\tilde{K})^{-1}\}\\ &=\mathcal{L}^{-1}\{(sI-A_p)^{-1}(sI-A_p+A_e+B_e\tilde{K})(sI-A_m-B_m\tilde{K})^{-1}\}\\ &=\mathcal{L}^{-1}\{(I+(sI-A_p)^{-1}(A_e+B_e\tilde{K}))(sI-A_m-B_m\tilde{K})^{-1}\}\\ &=\mathcal{L}^{-1}\{(sI-A_m-B_m\tilde{K})^{-1}+(sI-A_p)^{-1}(A_e+B_e\tilde{K})\\ &(sI-A_m-B_m\tilde{K})^{-1}\}=e^{(A_m+B_m\tilde{K})\delta_t}\\ &+e^{A_p\delta_t}\int_0^{\delta_t}e^{-A_pt}(A_e+B_e\tilde{K})e^{(A_m+B_m\tilde{K})t}dt.\end{aligned}$$

Then the nonzero eigenvalues of matrix $\mathcal{S}$ are the eigenvalues of matrix[23]

$$\mathcal{N}=e^{(A_m+B_m\tilde{K})\delta_t}+e^{A_p\delta_t}\int_0^{\delta_t}e^{-A_pt}(A_e+B_e\tilde{K})e^{(A_m+B_m\tilde{K})t}dt, \quad (27)$$

where $\mathcal{N}$ consists of two parts; the major term, $\mathcal{N}_m=e^{(A_m+B_m\tilde{K})\delta_t}$, and the perturbation term, $\mathcal{N}_e=e^{A_p\delta_t}\int_0^{\delta_t}e^{-A_pt}(A_e+B_e\tilde{K})e^{(A_m+B_m\tilde{K})t}dt$. The eigenvalues of $\mathcal{N}$ should be placed in a unit circle to satisfy the closed-loop stability requirement. The perturbation term depends on the updating period for snapshots (time interval between ROM revisions), δ_t, and the model mismatch. Also based on (27) we conclude that δ_t for a process depends on the controller gain, locations of the actuators and the model mismatch. Then we can ensure $\mathcal{N}_e \ll \mathcal{N}_m$ by choosing small values for δ_t or using more accurate models.

One way to find a criteria for δ_t based on closed-loop stability is by assuming an upper bound for the uncertain term as follows

$$\|\lambda^{\max}\{\mathcal{N}_e\}\|_2 \le \sigma, \quad (28)$$

where $\lambda^{\max}(\cdot)$ denotes the maximum eigenvalue of matrix $(\cdot)$ and σ is a small positive number. From Theorem 1, Eqs. 25–27 and triangular inequality we obtain

$$\|\lambda^{\max}\{\mathcal{N}_m+\mathcal{N}_e\}\|_2 \le \|\lambda^{\max}\{\mathcal{N}_m\}\|_2+\|\lambda^{\max}\{\mathcal{N}_e\}\|_2 < 1. \quad (29)$$

Using (28), we have

$$\|\lambda^{\max}\{\mathcal{N}_m\}\|_2=\|\lambda^{\max}\{e^{(A_m+B_m\tilde{K})\delta_t}\}\|_2 < 1-\sigma. \quad (30)$$

Finally, the above inequality can be presented as follows,

$$\log_{10}\left(\|\lambda^{\max}\{e^{(A_m+B_m\tilde{K})\delta_t}\}\|_2\right) < \log_{10}(1-\sigma) < 0. \quad (31)$$

Then by tracking $\lambda^{\max}$ for different values of δ_t, the δ_t values can be found that satisfy the system closed-loop stability. Note that considering $\log_{10}(\|\lambda^{\max}\{\mathcal{N}_m\}\|_2) < 0$ gives us an idea of δ_t values for the error-free case.

Another approach to identify an upper bound for δ_t considering closed-loop stability can be presented by setting upper bounds for open-loop and closed-loop model uncertainty. We know that for matrix $\mathcal{N}$

$$\|\lambda^{\max}\{\mathcal{N}\}\|_2 \le \sigma^{\max}\{\mathcal{N}\}=\|\mathcal{N}\|_2, \quad (32)$$

where $\sigma^{\max}(\cdot)$ denotes the maximum singular value of matrix $(\cdot)$. Then using (27) we obtain

$$\begin{aligned}\|\mathcal{N}\|_2&=\|e^{(A_m+B_m\tilde{K})\delta_t}+e^{A_p\delta_t}\int_0^{\delta_t}e^{-A_pt}(A_e+B_e\tilde{K})e^{(A_m+B_m\tilde{K})t}dt\|_2\\ &\le \|e^{(A_m+B_m\tilde{K})\delta_t}\|_2+\|e^{A_p\delta_t}\int_0^{\delta_t}e^{-A_pt}(A_e+B_e\tilde{K})e^{(A_m+B_m\tilde{K})t}dt\|_2.\end{aligned} \quad (33)$$

From this point, we consider two cases based on the stability or instability of the open-loop process:

Case I. *open-loop process is unstable*

$$\begin{aligned}&\left\|e^{(A_m+B_m\tilde{K})\delta_t}\right\|_2+\left\|e^{A_p\delta_t}\int_0^{\delta_t}e^{-A_pt}(A_e+B_e\tilde{K})e^{(A_m+B_m\tilde{K})t}dt\right\|_2\\ &\le \left(\left\|e^{A_m^{\mathrm{cl}}}\right\|_2\right)^{\delta_t}+e^{\tilde{\sigma}_1\delta_t}\left\|\int_0^{\delta_t}e^{-A_pt}\|A_e+B_e\tilde{K}\|_2e^{(A_m+B_m\tilde{K})t}dt\right\|_2\\ &\le \left(\left\|e^{A_m^{\mathrm{cl}}}\right\|_2\right)^{\delta_t}+e^{\tilde{\sigma}_1\delta_t}(\tilde{\sigma}_1+||A_m||_2+(\tilde{\sigma}_2+||B_m||_2)||\tilde{K}||_2)\\ &\left\|\int_0^{\delta_t}e^{(A_m^{\mathrm{cl}}-A_p)t}dt\right\|_2=\left(\left\|e^{A_m^{\mathrm{cl}}}\right\|_2\right)^{\delta_t}\\ &+\Sigma\frac{e^{\tilde{\sigma}_1\delta_t}}{||A_m+B_m\tilde{K}-A_p||_2}\left\|e^{(A_m^{\mathrm{cl}}-A_p)\delta_t}-1\right\|_2\\ &\le \left(\left\|e^{A_m^{\mathrm{cl}}}\right\|_2\right)^{\delta_t}+\Sigma\frac{e^{\tilde{\sigma}_1\delta_t}}{\left|\|A_m^{\mathrm{cl}}\|_2-\tilde{\sigma}_1\right|}\left\|e^{(A_m^{\mathrm{cl}}-A_p)\delta_t}-1\right\|_2<1\end{aligned} \quad (34)$$

where $A_m^{\mathrm{cl}}=A_m+B_m\tilde{K}$, $||A_p||_2 \le \tilde{\sigma}_1$, $||B_p||_2 \le \tilde{\sigma}_2$ and $\Sigma=\tilde{\sigma}_1+||A_m||_2+(\tilde{\sigma}_2+||B_m||_2)||\tilde{K}||_2$. If we assume that $e^{(A_m^{\mathrm{cl}}-A_p)\delta_t}\approx 0$ (from the fact that the open-loop process is unstable and by designing the controller gain), we obtain

$$\begin{aligned}&\left(\left\|e^{A_m^{\mathrm{cl}}}\right\|_2\right)^{\delta_t}+\Sigma\frac{e^{\tilde{\sigma}_1\delta_t}}{|\|A_m^{\mathrm{cl}}\|_2-\tilde{\sigma}_1}<1 \Rightarrow \delta_t\left[\ln\left(\left\|e^{A_m^{\mathrm{cl}}}\right\|_2\right)+\tilde{\sigma}_1\right]\\ &+\ln(\Sigma)-\ln(|\|A_m^{\mathrm{cl}}\|_2-\tilde{\sigma}_1|)<0\\ &\Rightarrow \delta_t<\frac{\ln\left(|\|A_m^{\mathrm{cl}}\|_2-\tilde{\sigma}_1|/\Sigma\right)}{\ln\left(\|e^{A_m^{\mathrm{cl}}}\|_2\right)+\tilde{\sigma}_1}=\delta_t^*\end{aligned} \quad (35)$$

Case II. *open-loop process is stable*

$$\begin{aligned}&\|e^{(A_m^{\mathrm{cl}})\delta_t}\|_2+\|e^{A_p\delta_t}\int_0^{\delta_t}e^{-A_pt}(A_e+B_e\tilde{K})e^{(A_m+B_m\tilde{K})t}dt\|_2\\ &\le \left(\|e^{A_m^{\mathrm{cl}}}\|_2\right)^{\delta_t}+\tilde{\sigma}_3\|\int_0^{\delta_t}e^{-A_pt}||A_e+B_e\tilde{K}||_2e^{(A_m^{\mathrm{cl}})t}dt\|_2\\ &\le \left(\|e^{A_m^{\mathrm{cl}}}\|\right)_2^{\delta_t}+\Sigma\frac{\tilde{\sigma}_3}{|\|A_m^{\mathrm{cl}}\|-\tilde{\sigma}_1|}\|e^{(A_m^{cl}-A_p)\delta_t}-1\|_2<1\end{aligned} \quad (36)$$

where $\|e^{A_p\delta_t}\|_2 \le \tilde{\sigma}_3$. If we assume that $e^{(A_m^{\mathrm{cl}}-A_p)\delta_t}\approx 0$ (by designing the controller gain), we obtain

$$\begin{aligned}&\left(\|e^{A_m^{\mathrm{cl}}}\|_2\right)^{\delta_t}+\frac{\Sigma\tilde{\sigma}_3}{|\|A_m^{\mathrm{cl}}\|_2-\tilde{\sigma}_1|}<1 \Rightarrow \delta_t\ln\left(\|e^{A_m^{\mathrm{cl}}}\|\right)_2\\ &+\ln(\Sigma\tilde{\sigma}_3)-\ln\left(|\|A_m^{\mathrm{cl}}\|_2-\tilde{\sigma}_1|\right)<0\\ &\Rightarrow \delta_t<\frac{\ln\left(\left|\|A_m^{\mathrm{cl}}\|_2-\tilde{\sigma}_1\right|/(\Sigma\tilde{\sigma}_3)\right)}{\ln\left(\|e^{A_m^{\mathrm{cl}}}\|_2\right)}=\delta_t^{**}\end{aligned} \quad (37)$$

Theorem 2. *Consider the dissipative, input-affine, linear PDE system of* (1) *for which Assumptions 1–2 always hold and Assumption 3 holds for finite periods between revisions. Also consider the infinite-dimensional representation of* (5) *and finite dimensional approximation of* (12) *in subspace* $\mathbb{P}$ *with APOD-based empirical basis functions. Under Assumptions of 1–3, the networked control strategy asymptotically stabilizes the system of* (1) *when the time interval between ROM updates,* δ_t*, is finite and larger than a critical value,* t_b*.*

Proof. Under Assumption 1 (time scale separation part), the system of (8) can be expressed in the following singular perturbation form

$$\dot{\bar{x}}_s = A_s\bar{x}_s + B_s\tilde{K}x_m, \quad \gamma\dot{\bar{x}}_f = \gamma A_f\bar{x}_f + \gamma B_f\tilde{K}x_m, \tag{38}$$

where $\gamma = |\lambda_1|/|\lambda_{\alpha+1}|$ is a small number that indicates the separation between the dominant and nondominant modes.[7] Due to the definition of A_f and γ, $A_{f\gamma} = \gamma A_f$ has negative eigenvalues of O(1) and based on controller design, the manipulating term in the fast subsystem, $B_f\tilde{K}x_m$, does not contain terms of $O(\frac{1}{\gamma})$ locally, where $O(\cdot)$ indicates the order of $(\cdot)$. By defining $\tau = t/\gamma$ and setting $\gamma = 0$, the fast subsystem dynamics of (38) can be expressed in the following fast time scale form

$$\frac{\partial\bar{x}_f}{\partial\tau} = A_{f\gamma}\bar{x}_f. \tag{39}$$

Then the solution of the locally exponentially stable system of (39) is obtained as

$$\bar{x}_f(\tau) = \bar{x}_f(0)e^{A_{f\gamma}\tau}. \tag{40}$$

Focusing on the norm of x_f, from (40) and Schwartz inequality we obtain

$$||\bar{x}_f(\tau)||_2 = ||\bar{x}_f(0)e^{A_{f\gamma}\tau}||_2 \le ||\bar{x}_f(0)||_2||e^{A_{f\gamma}\tau}||_2. \tag{41}$$

The definition of $A_{f\gamma}$ and the eigenspectrum bound to the fast subsystem imply that

$$||\bar{x}_f(0)||_2||e^{A_{f\gamma}\tau}||_2 \le ||\bar{x}_f(0)||_2 e^{(\gamma\lambda_{\alpha+1})\tau}, \tag{42}$$

where $\lambda_{\alpha+1}$ represents the dominant eigenvalue of A_f which is the least negative and of $O(\frac{1}{\gamma})$. Using singular perturbation arguments for infinite-dimensional systems it is shown that within a finite time the fast system dynamics will relax to a ball of radius $O(\gamma)$ around zero.[39] Using the spectral bound of (41) and (42) for the dynamic behavior and that $\gamma = |\lambda_1|/|\lambda_{\alpha+1}|$ we can obtain

$$||\bar{x}_f(0)||_2 e^{(\gamma\lambda_{\alpha+1})\tau} = ||x_f(0)||_2 e^{-|\lambda_1|\tau} \le O(\gamma); \tag{43}$$

this bound is satisfied when

$$\tau_b = \frac{t_b}{\gamma} \ge -\frac{1}{|\lambda_1|}\ln\left[O\left(\frac{\gamma}{||\bar{x}_f(0)||_2}\right)\right]. \tag{44}$$

We denote t_b with the time period needed by the fast dynamics of the process to stabilize and converge to a small neighborhood of zero

$$t_b \ge \frac{1}{|\lambda_{\alpha+1}|}\ln\left[O\left(\frac{||\bar{x}_f(0)||_2}{|\lambda_1|}|\lambda_{\alpha+1}|\right)\right]. \tag{45}$$

Considering t_b and the time interval between snapshots, $\delta_t = t_k - t_{k-1}$, we choose δ_t such that $\delta_t > t_b$. Then the infinite-dimensional system in (38) approximately reduces to the finite-dimensional slow system

$$\dot{\bar{x}}_s = A_s\bar{x}_s + B_s\tilde{K}x_m, \tag{46}$$

and the complete system of (13) reduces to

$$\begin{aligned} &\text{Process}: \dot{\bar{x}}_s = A_s\bar{x}_s + B_s u,\\ &\text{Model}: \dot{x}_m = A_m x_m + B_m u,\\ &\text{Controller}: u = \tilde{K}x_m. \end{aligned} \tag{47}$$

Then by considering Assumption 3 and based on the stable static state feedback control law, we conclude that the controller can stabilize the reduced order dynamics of (47). At this point, we know that the previous statement is true if and only if Assumptions 1, 2, and 3 hold. Focusing on the system dynamics Assumption 1 holds. Assumption 3 is satisfied for finite periods longer than the critical period of t_b. From this assumption we can assume that any basis functions of the slow subsystem are expressed in $\mathbb{P}\oplus\mathbb{Q}$. This assumption is not satisfied when new trends appear during the process evolution for the first time that makes the set of basis functions incomplete and the ROM inaccurate. Within a finite amount of time from when it happens, the APOD algorithm revises the basis functions and corrects the ROM. Following that, the controller is redesigned to retain relevancy. This procedure is recursively repeated during system progression to enforce closed-loop stability.

In Figure 2 the closed-loop process is presented under the proposed control structure in a block diagram form. ■

Remark 5. *Using the concept of settling time for linear systems we can relax the assumption of absence of $O(\frac{1}{\gamma})$ in the controller term and obtain a conservative estimate of t_b without considering singular perturbations arguments. The solution of fast mode dynamics of the system can be presented as*

$$\dot{\bar{x}}_f = A_f\bar{x}_f + B_f\tilde{K}x_m \Rightarrow \bar{x}_f(t) = e^{A_f t}\bar{x}_f(0) + \int_0^t e^{A_f(t-s)}B_f\tilde{K}x_m ds.$$

We can find the final value of the fast modes as follows

$$\lim_{t\to\infty}\bar{x}_f = \bar{x}_{f,ss} = -A_f^{-1}B_f\tilde{K}x_m.$$

Considering the settling time when the fast modes of the system reach within a 1% region of their final value, we obtain

$$\left|\frac{||\bar{x}_f(t_b)||_2 - ||\bar{x}_{f,\mathrm{ss}}||_2}{||\bar{x}_{f,\mathrm{ss}}||_2}\right| \le 0.01.$$

Using triangular inequality we can simplify the inequality as follows

$$\left|\frac{||\bar{x}_f(t_b)||_2 - ||\bar{x}_{f,\mathrm{ss}}||_2}{||\bar{x}_{f,\mathrm{ss}}||_2}\right| \le \frac{||\bar{x}_f(t_b) - \bar{x}_{f,\mathrm{ss}}||_2}{||\bar{x}_{f,\mathrm{ss}}||_2} \le 0.01.$$

From the above inequality we obtain

$$\frac{\|e^{A_f t_b}\bar{x}_f(0) + \int_0^{t_b} e^{A_f(t_b - T)}B_f\tilde{K}x_m dT + A_f^{-1}B_f\tilde{K}x_m\|_2}{||A_f^{-1}B_f\tilde{K}x_m||_2} \le 0.01.$$

If we assume that x_m does not change sharply during the time period of $[0, t_b]$ then using Cauchy-Schwarz and triangular inequalities we can simplify the problem as follows

$$\begin{aligned} &\frac{\|e^{A_f t_b}\bar{x}_f(0) + \int_0^{t_b} e^{A_f(t_b - T)}B_f\tilde{K}x_m dT + A_f^{-1}B_f\tilde{K}x_m\|_2}{||A_f^{-1}B_f\tilde{K}x_m||_2}\\ &= \frac{\|e^{A_f t_b}\bar{x}_f(0) + \left(\int_0^{t_b} e^{A_f(t_b - T)}dT\right)B_f\tilde{K}x_m + A_f^{-1}B_f\tilde{K}x_m\|_2}{||A_f^{-1}B_f\tilde{K}x_m||_2}\\ &= \frac{\|e^{A_f t_b}(\bar{x}_f(0) + A_f^{-1}B_f\tilde{K}x_m)\|_2}{||A_f^{-1}B_f\tilde{K}x_m||_2}\\ &\le \frac{||e^{A_f t_b}||_2(||\bar{x}_f(0)||_2 + ||A_f^{-1}B_f\tilde{K}x_m||_2)}{||A_f^{-1}B_f\tilde{K}x_m||_2} \le 0.01. \end{aligned}$$

Now we can solve the above inequality for t_b

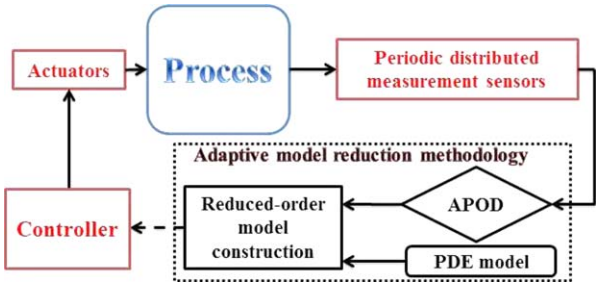

Figure 2. Process operation block diagram under proposed controller structure.

Red signifies the controller system. [Color figure can be viewed in the online issue, which is available at wileyonlinelibrary.com.]

$$||e^{A_f t_b}||_2\left(\frac{||\bar{x}_f(0)||_2}{||A_f^{-1}B_f\tilde{K}x_m||_2}+1\right)\le 0.01 \Rightarrow ||e^{A_f t_b}||_2 \le \frac{0.01}{\frac{||\bar{x}_f(0)||_2}{||A_f^{-1}B_f\tilde{K}x_m||_2}+1} \Rightarrow e^{-||\lambda_{\alpha+1}||_2 t_b} \le \frac{0.01}{\frac{||\bar{x}_f(0)||_2}{||A_f^{-1}B_f\tilde{K}x_m||_2}+1} \Rightarrow t_b \ge \frac{1}{||\lambda_{\alpha+1}||_2}\left[4.605+\ln\left(\frac{||\bar{x}_f(0)||_2}{||A_f^{-1}B_f\tilde{K}x_m||_2}+1\right)\right].$$

Remark 6. *The maximum allowable time interval between snapshots being communicated from the periodic spatially distributed measurement sensors to the model reduction and control structure is less than (a) the minimum time interval from* (31) *and* δ_t^* *for unstable open-loop process, (b) the minimum time interval from* (31) *and* δ_t^{**} *for stable open-loop process.*

Remark 7. *To identify the criterion presented in* (31), (35), *and* (37), *we have to find an upper bound for process operators,* A_p *and* B_p, *otherwise we can not determine criteria for* δ_t. *Considering* $A_p=A_e+A_m$ *and* $B_p=B_e+B_m$ *we obtain that* $||A_p||_2 \le ||A_e||_2+||A_m||_2$ *and* $||B_p||_2 \le ||B_e||_2+||B_m||_2$. *Note that the upper bounds of modeling error operators,* $||A_e||_2$ *and* $||B_e||_2$, *always converge to small neighborhood around zero using recursive POD methods (like APOD) during process evolution as more dynamical modes of the system are excited. Thus, an approximate upper bound of* $||A_e||_2$ *and* $||B_e||_2$ *can be obtained via subspace* $\mathbb{Q}$. *Then we may implement the summation of upper bounds of the empirical and modeling error operators in* (31), (35), *and* (37), *specifically for diffusion-reaction processes when the fast modes of the system converges to zero after a short period of time.*

Remark 8. *Based on the presented analysis one may encounter cases when* $t_b > \delta_t^*$ *which implies that the proposed procedure can not be used to regulate the system. This hurdle is surpassed by increasing* ξ *in APOD* [12] *which increases the dimensionality of the slow system and thus considers faster settling times,* t_b.

Remark 9. *For finite periods longer than the critical period of* t_b, *basis functions of the slow subsystem belong in* $\mathbb{P}\oplus\mathbb{Q}$. *The relative significance of the empirical eigenvalues is a strong indicator that the slow subsystem is included in* $\mathbb{P}\oplus\mathbb{Q}$. *Assumption 3 has two restrictions; the snapshot frequency is considered to be of the same order as magnitude of the dominant dynamics frequency and the slow dynamics are sufficiently excited.*[18] *The appearance of new trends in the system dynamics during process evolution is the main reason that Assumption 3 conditions are violated because they make the empirical basis functions and ROM inaccurate. When the conditions of this assumption are violated the APOD algorithm revises the set of empirical basis functions and modifies the ROM. Furthermore, the controller is redesigned to retain relevancy. Such "corrections" will always be repeated at revision times to enforce closed-loop stability.*

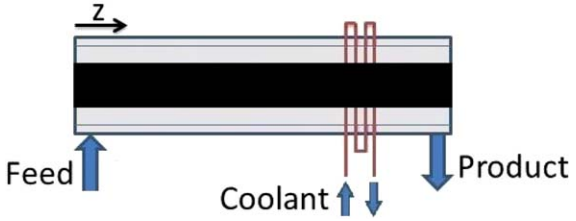

Figure 3. Tubular chemical reactor with cooling spiral at $z=0.75L$.

[Color figure can be viewed in the online issue, which is available at wileyonlinelibrary.com.]

Simulation Results

In this section, the proposed method is illustrated on temperature regulation of a tubular reactor. We considered a tubular chemical reactor shown in Figure 3, where an irreversible exothermic reaction of zeroth order with reaction rate, R, took place and a cooling jacket was used to remove heat from the reactor. We assumed constant physical properties and considered only the temperature. We studied two cases; (1) constant reaction rate and (2) Arrhenius dependence of the reaction rate to temperature.

Constant reaction rate

We considered an energy balance along the reactor length where the reaction rate was constant, $R = R_0$, as follows

$$\frac{\partial T}{\partial t}=\frac{k}{\rho c_p}\frac{\partial^2 T}{\partial z^2}-v\frac{\partial T}{\partial z}+\frac{(-\Delta H)}{\rho c_p}R_0-\frac{hA_s}{\rho c_p}b(z)(T-T_c), \quad (48)$$

with boundary conditions

$$z=0:\ \frac{\partial T}{\partial z}=\frac{\rho c_p v}{k}(T-T_f), \qquad z=L:\ \frac{\partial T}{\partial z}=0, \quad (49)$$

and initial condition

$$t=0:\ T=T_f. \quad (50)$$

In Eqs. 48–50, T is the reactor temperature, t is time and $z \in [0, L]$ is the spatial domain. k, ρ, and c_p denote the thermal conductivity, density and heat capacity of the fluid inside the reactor, respectively. v is the axial fluid velocity, h is heat transfer coefficient between the reactor and the cooling jacket and A_s is the surface area of the reactor walls. Also $b(z)$ describes the location of the cooling jacket and $(-\Delta H)$ denotes the heat of the reaction.

By considering the steady-state temperature

$$\frac{k}{\rho c_p}\frac{\partial^2 T_{ss}}{\partial z^2}-v\frac{\partial T_{ss}}{\partial z}+\frac{(-\Delta H)}{\rho c_p}R_0-\frac{hA_s}{\rho c_p}b(z)(T_{ss}-T_{c,ss})=0, \quad (51)$$

subject to the following boundary conditions

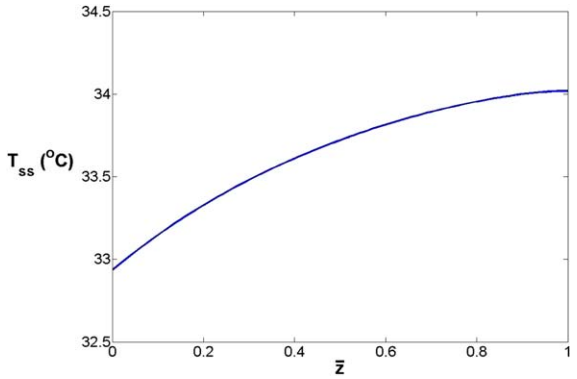

Figure 4. The desired spatial profile of steady-state temperature.

[Color figure can be viewed in the online issue, which is available at wileyonlinelibrary.com.]

$$z=0: \frac{dT_{ss}}{dz}=\frac{\rho c_p v}{k}(T_{ss}-T_f),$$
$$z=L: \frac{dT_{ss}}{dz}=0, \tag{52}$$

the following equations can be obtained from the system of (48)–(50)

$$\frac{\partial \bar{T}}{\partial \bar{t}}=\frac{1}{Pe}\frac{\partial^2 \bar{T}}{\partial \bar{z}^2}-\frac{\partial \bar{T}}{\partial \bar{z}}-\beta b(\bar{z})\bar{T}+\beta b(\bar{z})u \tag{53}$$

$$\bar{z}=0: \frac{\partial \bar{T}}{\partial \bar{z}}=Pe\bar{T},$$
$$\bar{z}=1: \frac{\partial \bar{T}}{\partial \bar{z}}=0, \tag{54}$$

$$\bar{t}=0: \bar{T}=\bar{T}_f, \tag{55}$$

where the dimensionless variables and parameters are defined as follows

$$\bar{T}=\frac{T-T_{ss}}{T_{ss}},\ \bar{T}_f=\frac{T_f-T_{ss}}{T_{ss}},\ u=\frac{T_c-T_{c,ss}}{T_{ss}},\ \bar{z}=\frac{z}{L},$$
$$\mathrm{Pe}=\frac{\rho c_p v L}{k},\ \beta=\frac{hA_s L}{\rho c_p v},\ \bar{t}=\frac{tv}{L}. \tag{56}$$

We considered Pe = 7, $\bar{T}_f=-0.3$ and $\beta=2$ for the parameters in process system of (53)–(55). One control actuator was assumed to be available at $\mathcal{L}_a=0.75$ in the spatial domain $\bar{z}=[0,1]$ and the corresponding spatial distribution function at the actuator location was $b(\bar{z})=\delta(\bar{z}-\mathcal{L}_a)$ that indicates point actuation ($\delta(\cdot)$ denotes the standard Dirac delta function). Figure 4 presents the steady-state temperature where $T_f=17°\mathrm{C}, T_{c,ss}=27°\mathrm{C}$ and $\gamma=\frac{(-\Delta H)}{\rho c_p v}R_0 L=15$. This temperature profile is the desired basis for the regulation problem.

As the availability of snapshots of the process is usually limited, to obtain δ_t, we initially simulated the open-loop process for the time period of $\bar{t}=[0,2]$. We obtained 20 snapshots during this open-loop period, then we computed the initial basis functions by applying the off-line APOD to the ensemble of snapshots. This off-line procedure resulted in two empirical basis functions for $\bar{T}$ which captured 0.99 of the energy embedded in the ensemble. The APOD model was derived using the empirical basis functions and Galerkin's projection, that is, A_m and B_m were obtained. Then we computed $t_b=0.2$ from (45) and the open-loop simulation

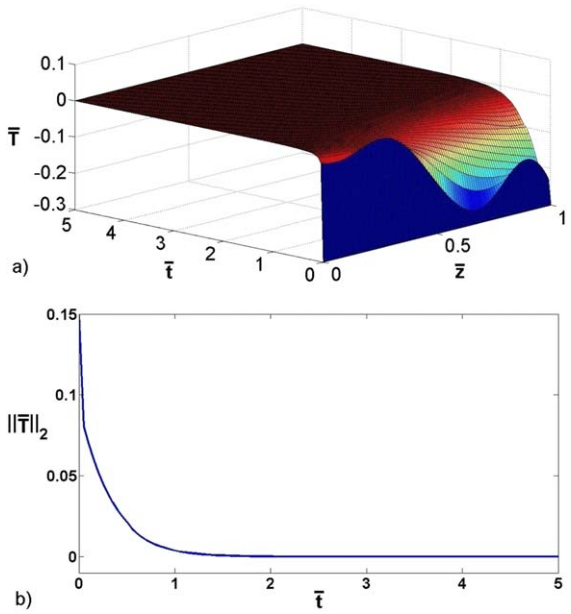

Figure 5. Closed-loop system temporal profile of (a) the deviation state spatial profile and (b) norm of the deviation state.

[Color figure can be viewed in the online issue, which is available at wileyonlinelibrary.com.]

results. Note that t_b must be considered as a lower bound for δ_t. Considering $\sigma=0.05$, the initial upper bound of δ_t was computed based on (31) where $\tilde{K}=0$ ($\delta_t \leq 0.67$). We chose the initial value of δ_t using such lower and upper bounds.

During the closed-loop process evolution assuming $||A_p||_2 \approx ||A_m||_2$ and $||B_p||_2 \approx ||B_m||_2$, we set $\tilde{\sigma}_1=||A_m||_2$ and $\tilde{\sigma}_2=||B_m||_2$. Then we computed $\Sigma=\tilde{\sigma}_1+||A_m||_2+(\tilde{\sigma}_2+||B_m||_2)||\tilde{K}||_2$. The parameter $\tilde{\sigma}_3$ was also adjusted at the value of 1 considering $\delta_t>0$ and $\lambda(A_p)<0$. The value of δ_t^{**} was computed from (37) (where the smallest value of δ_t^{**} was equal to 0.63 as time evolved). The final value of δ_t at each revision was identified based on Remark 6 considering t_b as the lower bound.

Considering the above discussion, we adjusted the sampling frequency of snapshots of the process at every $\delta_t=0.5$ units of time during closed-loop operation. This value satisfied all criteria. We can change δ_t during process evolution, however we only considered a constant value in this example for simplicity reasons. Figure 5 presents the temporal profile of closed-loop process and its two-norm, respectively. We observe that the controller successfully stabilized the system of (53)–(55) at $\bar{T}(\bar{z},\bar{t})=0$, as the process profile and its norm converged to zero without any peaking.

Figure 6 shows the temporal profile of required control action, the dominant mode estimated using APOD and the norm of error between the process and the ROM. To compute the controller gain we placed the first closed-loop pole at -5 (for $r=1,\ 2$) and the second closed-loop pole at -7 (for $r=2$). The control action converged to zero and we did not observe any chattering. The mode of the system converged to zero which illustrates the effectiveness of the proposed controller structure to stabilize the system. The success of the designed controller in regulating the process was due to the dominant subspace (hence the ROM and the control law) being updated as the process traverses through different regions of the state space during closed-loop operation. Figure

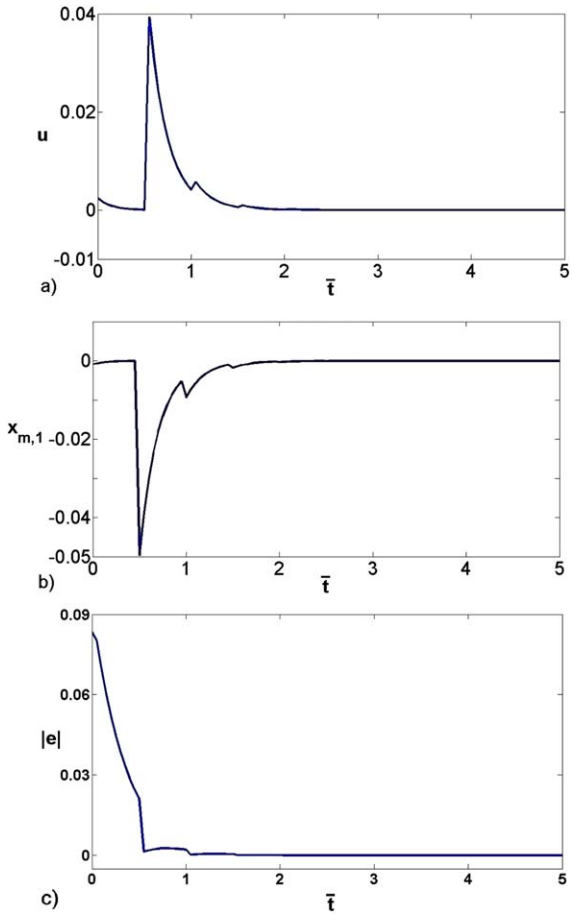

Figure 6. Temporal profile of (a) control action, (b) dominant estimated mode, and (c) norm of error between the process and the ROM.

[Color figure can be viewed in the online issue, which is available at wileyonlinelibrary.com.]

7 presents the change of number of basis functions. During the closed-loop process operation, when new trends appeared the dominant subspace basis was updated to accurately capture the process behavior, appropriately changing the number of empirical basis functions. Note that the system is linear and there are no basic dynamic behavior changes; the only reason for changes in the ROM dynamics as time evolved was the erroneous ordering of the empirical basis functions since the specific modes can be locally close to zero during initial sampling. Figure 8 presents the temporal profile of the

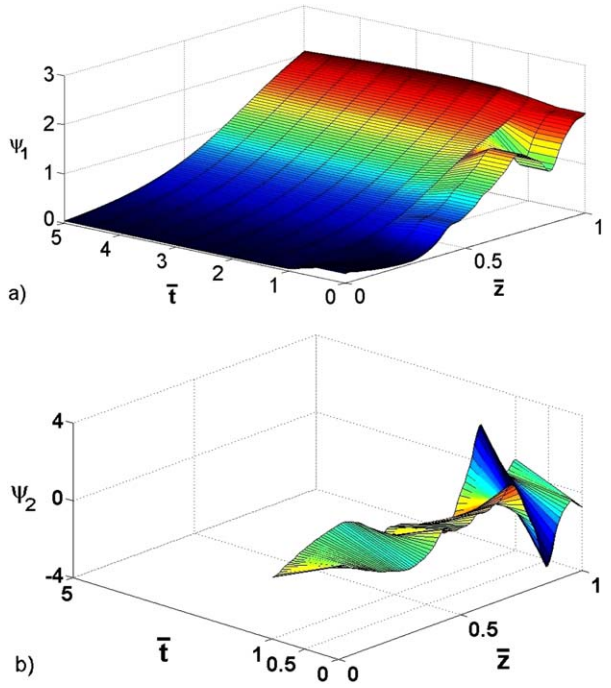

Figure 8. Temporal profile of the (a) first and (b) second empirical basis functions.

[Color figure can be viewed in the online issue, which is available at wileyonlinelibrary.com.]

dominant empirical basis functions. Note that the second empirical basis function only existed during the time period of [0,1]. It was observed that the basis function was adapting itself with the system during the process evolution.

There is always a trade-off between stability satisfaction and ROM revision load based on the value of δ_t. Larger values of δ_t reduce the computation load for ROM updates but lead to loss of closed-loop stability. Figure 9 compares the logarithmic temporal profiles of $||\lambda^{\max}\{\mathcal{N}_m\}||_2$ for different values of δ_t. Based on the criteria of (30) for $\sigma=0.05$, the value of δ_t that satisfies $\log_{10}(||\lambda^{\max}\{\mathcal{N}_m\}||_2) \leq -0.02$ at steady state had to been chosen; this means the previously chosen value of δ_t satisfied the system closed-loop stability requirements.

Temperature dependent reaction rate

To illustrate the importance of choosing the correct time interval for ROM revisions of open-loop unstable linearized DPSs we then focused on regulating the thermal dynamics in

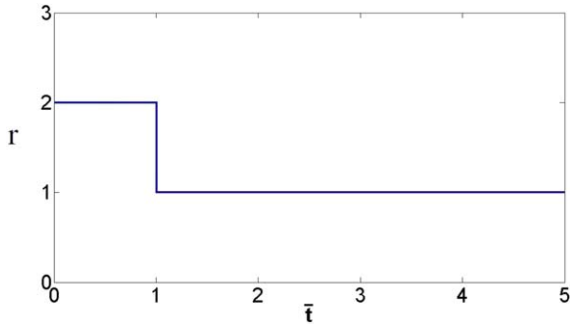

Figure 7. Number of basis functions.

[Color figure can be viewed in the online issue, which is available at wileyonlinelibrary.com.]

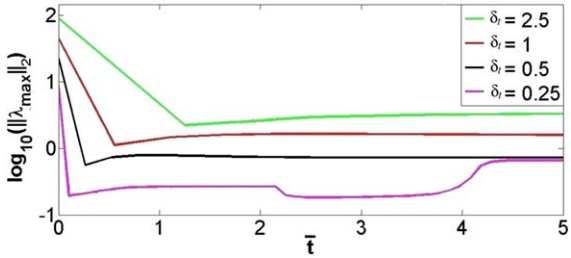

Figure 9. Temporal profile of absolute value of maximum characteristic eigenvalue for different ROM updating period times.

[Color figure can be viewed in the online issue, which is available at wileyonlinelibrary.com.]

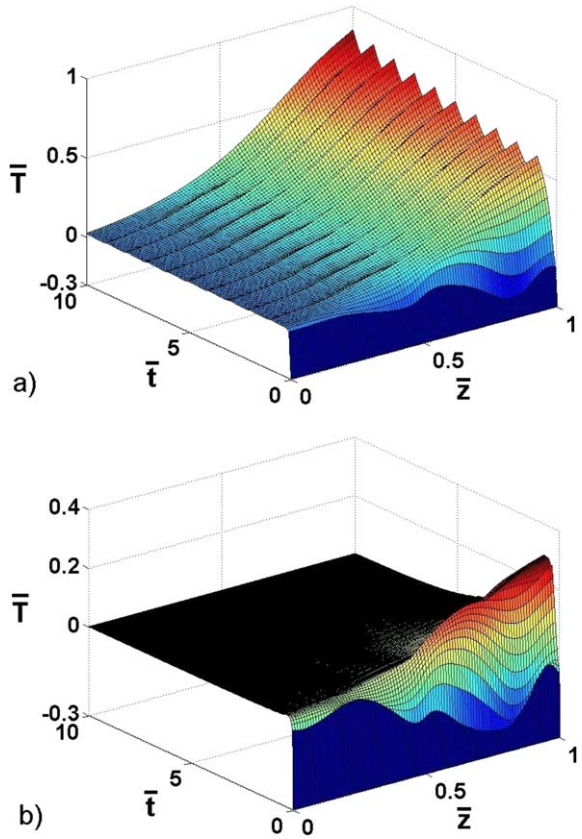

Figure 10. Closed-loop spatiotemporal profile of the system for (a) δ_t=1 and (b) δ_t=0.4.

[Color figure can be viewed in the online issue, which is available at wileyonlinelibrary.com.]

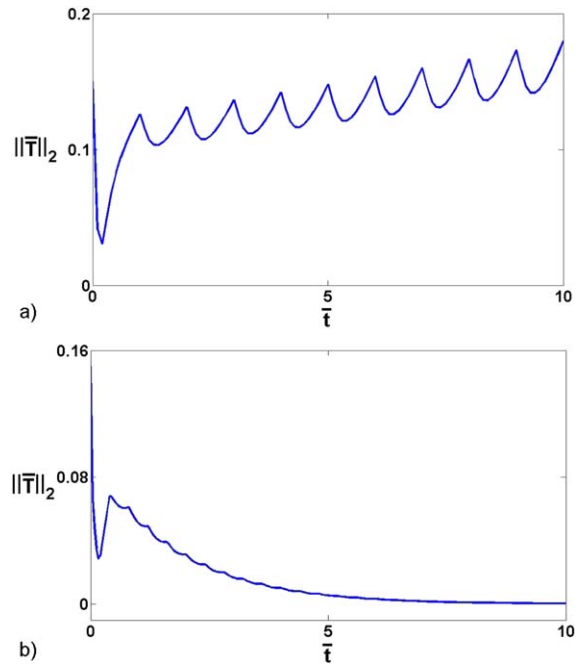

Figure 11. Closed-loop temporal profile of the system two-norm for (a) δ_t=1 and (b) δ_t=0.4.

[Color figure can be viewed in the online issue, which is available at wileyonlinelibrary.com.]

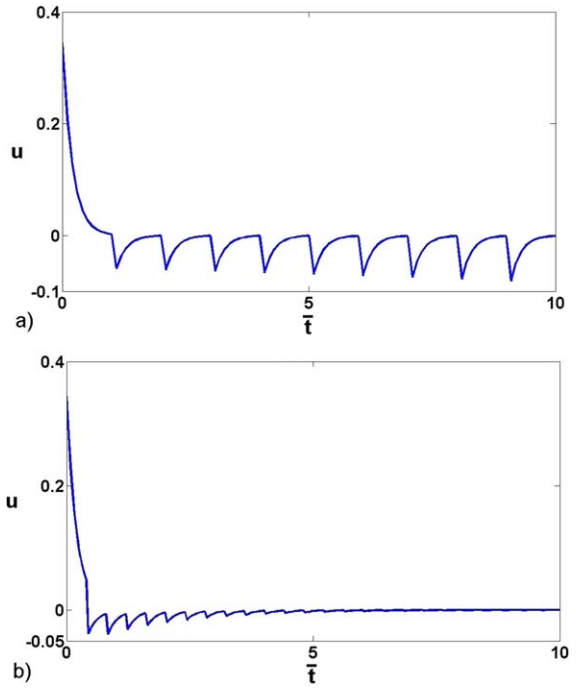

Figure 12. Temporal profile of required control action for (a) δ_t=1 and (b) δ_t=0.4.

[Color figure can be viewed in the online issue, which is available at wileyonlinelibrary.com.]

the same tubular reactor of the previous section when an irreversible exothermic reaction of zeroth order with Arrhenius temperature dependent reaction rate of $\tilde{R}_0 e^{-\frac{E}{RT}}$ takes place. The energy balance can then be presented in the following form

$$\frac{\partial T}{\partial t}=\frac{k}{\rho c_p}\frac{\partial^2 T}{\partial z^2}-v\frac{\partial T}{\partial z}+\frac{(-\Delta H)}{\rho c_p}\tilde{R}_0 e^{-\frac{E}{RT}}-\frac{hA_s}{\rho c_p}b(z)(T-T_c), \tag{57}$$

with the same boundary and initial conditions of (49)–(50), where E denotes the reaction activation energy and R is the universal gas constant. Considering the Taylor expansion of the nonlinear term, $e^{-\frac{E}{RT}}$, around an unstable steady state, T_{ss}, as

$$e^{-\frac{E}{RT}}\approx e^{-\frac{E}{RT_{ss}}}\left(1+\frac{E}{RT_{ss}^2}(T-T_{ss})\right),$$

we obtained the linearized PDE system of

$$\frac{\partial T}{\partial t}=\frac{k}{\rho c_p}\frac{\partial^2 T}{\partial z^2}-v\frac{\partial T}{\partial z}+\frac{(-\Delta H)}{\rho c_p}\tilde{R}_0 e^{-\frac{E}{RT_{ss}}}\left(1+\frac{E}{RT_{ss}^2}(T-T_{ss})\right)-\frac{hA_s}{\rho c_p}b(z)(T-T_c). \tag{58}$$

Accordingly, the spatial profile of the unstable steady-state temperature took the following form

$$\frac{k}{\rho c_p}\frac{\partial^2 T_{ss}}{\partial z^2}-v\frac{\partial T_{ss}}{\partial z}+\frac{(-\Delta H)}{\rho c_p}\tilde{R}_0 e^{-\frac{E}{RT_{ss}}}-\frac{hA_s}{\rho c_p}b(z)(T_{ss}-T_{c,ss})=0, \tag{59}$$

with respect to the same boundary conditions of (52). Then we derived the following dimensionless PDE from (58)–(59)

$$\frac{\partial \bar{T}}{\partial \bar{t}}=\frac{1}{\mathrm{Pe}}\frac{\partial^2 \bar{T}}{\partial \bar{z}^2}-\frac{\partial \bar{T}}{\partial \bar{z}}+\hat{\beta}\bar{T}-\beta b(\bar{z})\bar{T}+\beta b(\bar{z})u$$
$$\bar{z}=0:\frac{\partial \bar{T}}{\partial \bar{z}}=\mathrm{Pe}\bar{T}, \tag{60}$$
$$\bar{z}=1:\frac{\partial \bar{T}}{\partial \bar{z}}=0,$$
$$\bar{t}=0:\bar{T}=\bar{T}_f,$$

where

$$\hat{\beta}=\frac{(-\Delta H)}{\rho c_p v}\tilde{R}_0 L\frac{E}{RT_{\mathrm{ss}}^2}e^{-\frac{E}{RT_{\mathrm{ss}}}}$$

subject to the dimensionless variables and parameters of (56).

We considered the same set of operation parameters as in the previous section (Pe = 7, $\bar{T}_f=-0.3$ and $\beta=2$). The reaction thermal source parameter was also considered as $\hat{\beta}=1.5$ in the simulation. An analysis of the open-loop process behavior showed that the spatially uniform steady state was now unstable. As a result the control objective became to regulate the process at the spatially uniform steady state of $\bar{T}=0$.

A single actuator was assumed to be available at $\mathcal{L}_a=0.75$ and the control and MOR strategy was the same as previous section. To obtain δ_t, we initially simulated the open-loop process and computed the initial basis functions by applying the off-line APOD to the ensemble of snapshots. Then we obtained A_m and B_m from the APOD model. We thus computed the value of $t_b=0.1$ from the open-loop simulation results. The initial upper bound of δ_t was computed based on (31) ($\delta_t \leq 0.52$). We chose the initial value of δ_t using such lower and upper bounds. During the closed-loop process evolution by assuming $||A_p||_2 \approx ||A_m||_2$ and $||B_p||_2 \approx ||B_m||_2$, we set $\tilde{\sigma}_1=||A_m||_2$ and $\tilde{\sigma}_2=||B_m||_2$. Then we computed $\Sigma=\tilde{\sigma}_1+||A_m||_2+(\tilde{\sigma}_2+||B_m||_2)||\tilde{K}||_2$. The value of δ_t^* was computed from (35) (where the smallest value of δ_t^* was equal to 0.5 as time evolved). The final value of δ_t at each revision was identified based on Remark 6 considering t_b as the lower bound. We applied $\delta_t=1$ as the initial time interval between sampling snapshots and we compared it to $\delta_t=0.4$, that had been identified based on the criterion of (31) and (35). The controller structure performance for two different values of δ_t is presented in the Figures 10–12. Figure 10 compares the closed-loop spatiotemporal behavior of the dimensionless temperature for the two applied time intervals. The temporal profiles of the closed-loop system two-norm are presented in Figure 11, and Figure 12 shows the required control actions. We observe that the controller successfully stabilized the system of (60) at $\bar{T}(\bar{z},\bar{t})=0$ when $\delta_t=0.4$. We also observe that the sampling frequency of $\delta_t=1$ was insufficient to stabilize the plan, and the process exhibited an oscillatory behavior far away from the desired steady state (shown in Figures 10a and 11a). This was due to the control action (shown in Figure 12a) which was insufficient to drive the closed-loop system due to ROM inaccuracy.

The effectiveness of the proposed APOD-based control structure in stabilizing the linear process lies on the ROM revisions as the process passes through different regions of the state space domain. As we discussed in this article, such revisions had to be quite frequent to accurately capture the process behavior when new trends appeared during closed-loop operation.

Conclusion

Model-based controllers were designed for linear distributed processes based on restricted communication between the control system elements. We addressed the modeling component question via APOD algorithm to recursively compute the set of empirical basis functions. The problem with linear systems is that due to subsampling the empirical basis functions and modes may not be properly ordered. We used APOD to properly express the system while circumventing extensive off-line computations. The main objective was to minimize snapshots transfer rate from the distributed sensors to the controller, for ROM revisions, considering closed-loop stability. Based on the analysis, we identified a time interval bound that needs to be satisfied to preserve closed-loop stability. The proposed control structure was illustrated on the temperature regulation problem of a tubular reactor.

Acknowledgment

Financial support from the National Science Foundation, CMMI Award # 13–00322 is gratefully acknowledged.

Literature Cited

1. Armaou A, Christofides PD. Nonlinear feedback control of parabolic PDE systems with time-dependent spatial domains. *J Math Anal Appl*. 1999;239:124–157.
2. Christofides PD, Daoutidis P. Finite-dimensional control of parabolic PDE systems using approximate inertial manifolds. *J Math Anal Appl*. 1997;216:398–420.
3. Garcia MR, Vilas C, Santos LO, Alonso AA. A robust multi-model predictive controller for distributed parameter systems. *J Process Control*. 2012;22:60–71.
4. Smyshlyaev A, Krstic M. On control design for PDEs with space-dependent diffusivity or time-dependent reactivity. *Automatica*. 2005;41:1601–1608.
5. Balas MJ. Feedback control of linear diffusion processes. *Int J Control*. 1979;29:523–533.
6. Balas MJ. Nonlinear finite-dimensional control of a class of nonlinear distributed parameter systems using residual mode filters: A proof of local exponential stability. *J Math Anal Appl*. 1991;162:63–70.
7. Christofides PD. *Nonlinear and Robust Control of PDE Systems*. New York: Birkhäuser, 2000.
8. Demetriou MA, Smith RC. *Research Directions in Distributed Parameter Systems*. Philadelphia: SIAM Frontiers in Applied Mathematics, 2003.
9. Armaou A, Christofides PD. Finite-dimensional control of nonlinear parabolic PDE systems with time-dependent spatial domains using empirical eigenfunctions. *Int J Appl Math Comput Sci*. 2001;11:287–317.
10. Babaei Pourkargar D, Armaou A. Modification to adaptive model reduction for regulation of distributed parameter systems with fast transients. *AIChE J*. 2013;59(12):4595–4611.
11. Christofides PD, Armaou A. Global stabilization of the Kuramoto-Sivashinsky equation via distributed output feedback control. *Syst Control Lett*. 2000;39:283–294.
12. Pitchaiah S, Armaou A. Output feedback control of distributed parameter systems using adaptive proper orthogonal decomposition. *Ind Eng Chem Res*. 2010;49:10496–10509.
13. Sirovich L. Turbulence and the dynamics of coherent structures: Parts I, II and III. *Q Appl Math*. 1987;XLV:561–590.
14. Chinesta F, Ladeveze P, Cueto E. A short review on model order reduction based on proper generalized decomposition. *Arch Comput Methods Eng*. 2011;18:395404.
15. Dickinson BT, Singler JR. Nonlinear model reduction using group proper orthogonal decomposition. *Int J Numer Anal Model*. 2010;7(2):356–372.
16. Izadi M, Dubljevic S. Order-reduction of parabolic PDEs with time-varying domain using empirical eigenfunctions. *AIChE J*. 2013;59(11):4142–4150.

17. Samadiani E, Joshi Y. Reduced order thermal modeling of data centers via proper orthogonal decomposition: A review. *Int J Numer Methods Heat Fluid Flow*. 2010;20(5):529–550.
18. Varshney A, Pitchaiah S, Armaou A. Feedback control of dissipative distributed parameter systems using adaptive model reduction. *AIChE J*. 2009;55:906–918.
19. Babaei Pourkargar D, Armaou A. Control of dissipative partial differential equation systems using APOD based dynamic observer designs. In: *Proceedings of the American Control Conference*, Washington, DC, 2013:502–508.
20. Babaei Pourkargar D, Armaou A. Geometric output tracking of nonlinear distributed parameter systems via adaptive model reduction. *Chem Eng Sci*. 2014;116:418–427.
21. Babaei Pourkargar D, Armaou A. Output tracking of spatiotemporal thermal dynamics in transport-reaction processes via adaptive model reduction. In: *Proceedings of the American Control Conference*, Portland, OR, 2014:3352–3358.
22. Pitchaiah S, Armaou A. Output feedback control of dissipative PDE systems with partial sensor information based on adaptive model reduction. *AIChE J*. 2013;59(3):747–760.
23. Montestruque LA, Antsaklis P. On the model-based control of networked systems. *Automatica*. 2003;39:1837–1843.
24. Yao Z, El-Farra NH. Networked control of specially distributed processes using an adaptive communication policy. In: *Proceedings of the 49th IEEE Conference on Decision and Control*, Atlanta, GA, 2010.
25. Hespanha JP, Naghshtabrizi P, Xu Y. A survey of recent results in networked control systems. *Proc IEEE*. 2007;95(1):138–162.
26. Babaei Pourkargar D, Armaou A. Feedback control of linear distributed parameter systems via adaptive model reduction in the presence of device network communication constraints. In: *Proceedings of the American Control Conference*, Portland, OR, 2014:1667–1673.
27. Sun Y, Ghantasala S, El-Farra NH. Networked control of specially distributed processes with sensor-controller communication constraints. In: *Proceedings of the American Control Conference*, St. Louis, MO, 2009:2489–2494.
28. Yao Z, Sun S, El-Farra NH. Resource-aware scheduled control of distributed process systems over wireless sensor networks. In: *Proceedings of the American Control Conference*, Baltimore, MD, 2010: 4121–4126.
29. Christofides PD. Robust control of parabolic PDE systems. *Chem Eng Sci*. 1998;53(16):2949–2965.
30. Adomaitis RA. A reduced-basis discretization method for chemical vapor deposition reactor simulation. *Math Comput Model*. 2003; 38(1–2):159–175.
31. Lu P, Edgar JH, Glembocki OJ, Klein PB, Glaser ER, Perrin J, Chaudhuri J. High-speed homoepitaxy of SiC from methyltrichlorosilane by chemical vapor deposition. *J Cryst Growth*. 2005;285(4):506–513.
32. Theodoropoulou A, Adomaitis RA, Zafiriou E. Model reduction for optimization of rapid thermal chemical vapor deposition systems. *IEEE Trans Semicond Manuf*. 1998;11(1):85–98.
33. Lin YH, Adomaitis RA. Simulation and model reduction methods for an RF plasma glow discharge. *J Comput Phys*. 2001;171(2):731–752.
34. Friedland B. *Control System Design: An Introduction to State-Space Methods*. New York: McGraw-Hill, 2005.
35. Russell DL. Controllability and stabilizability theory for linear partial differential equations: Recent progress and open questions. *SIAM Rev*. 1978;20:639–739.
36. Armaou A, Demetriou MA. Optimal actuator/sensor placement for linear parabolic PDEs using spatial h-2 norm. *Chem Eng Sci*. 2006; 61(22):7351–7367.
37. Demetriou MA, Hussein II. Estimation of spatially distributed processes using mobile spatially distributed sensor network. *SIAM J Control Optim*. 2009;48(1):266–291.
38. Curtain RF, Zwart H. *An Introduction to Infinite-Dimensional Linear Systems Theory*. New York: Springer-Verlag, 1995.
39. Lobry C, Sari T, Touhami S. On Tykhonov's theorem for convergence of solutions of slow and fast systems. *Electron J Diff Equ*. 1998;1998(19):1–22.

Manuscript received May 19, 2014, and revision received Aug. 19, 2014.